

Modification of Ytria-doped Tetragonal Zirconia Polycrystal Ceramics

K. Obal, Z. Pedzich, T. Brylewski, M. Rekas*

AGH University of Science and Technology, Faculty of Materials Science and Ceramics, al. Mickiewicza 30, 30-059 Cracow, Poland

*E-mail: rekas@agh.edu.pl

Received: 19 June 2012 / *Accepted:* 14 July 2012 / *Published:* 1 August 2012

3 mol.% Y_2O_3 - ZrO_2 (3Y-TZP) powder was prepared using the coprecipitation method. The effects of adding various amounts of aluminum oxide to the 3Y-TZP and the influence of sintering temperature were studied. The best microstructural and electrical properties from the viewpoint of application as solid electrolytes were observed for the samples that contained 0.5 mol.% Al_2O_3 and were sintered at 1500°C.

Keywords: Tetragonal zirconia, Ionic conductivity, Grain boundary conductivity, Blocking effect , Impedance spectroscopy

1. INTRODUCTION

Oxygen-conducting solid electrolytes play an important role in technologies such as solid oxide fuel cells (SOFCs), oxygen sensors, oxygen electrochemical pumps and gas separators. The applied electrolyte should meet the following requirements:

- high electrical conductivity
- ionic transference number close to 1
- high mechanical strength
- high interfacial gas-solid reaction kinetics
- operating temperature that is not overly high
- long-term stability
- low material, manufacturing and maintenance costs

The first well-known oxygen-conducting solid electrolytes were zirconia-based materials, especially those belonging to the Y_2O_3 - ZrO_2 solid solutions. Within this system three types of materials may be applied as an engineering material: fully stabilized zirconia (FSZ), partially stabilized zirconia (PSZ) and tetragonal zirconia polycrystals (Y-TZP).

The first type (FSZ), which contains from 6 to 10 mol.% Y_2O_3 , has a cubic structure, and exhibits high ionic conductivity at elevated temperatures. Regardless of this advantage, its widespread commercial application is limited due to high operating temperatures (700-1000°C), low mechanical strength, and poor resistance to thermal shocks.

PSZ, which contains 4 to 5 mol.% Y_2O_3 , consists of a cubic and tetragonal phase mixture. It exhibits good mechanical strength and toughness [1]. However, its electrical properties are worse than that FSZ.

The third type, Y-TZP, with a 1 to 3 mol.% Y_2O_3 content, has a submicron tetragonal grain structure [2,3] and due to its very high mechanical strength (>1GPa) and fracture toughness (>4-6 $MPa \cdot m^{1/2}$) is named *ceramic steel* [4,5].

At moderate temperatures below 700°C the grain interior of Y-TZP has higher conductivity (σ_b) than that of fully (YSZ) or partially stabilized (PSZ) zirconia [6]. However, the total conductivity of Y-TZP is lower due to the high contribution of grain boundary resistivity, known as the blocking effect [7-9]. Specific grain boundary conductivity of yttria-doped zirconia is ca. 2 orders of magnitude lower than its bulk conductivity [10]. Generally, there are two causes of the blocking effect.

The first cause is related to the presence of impurities, mainly silicon, that are segregated on grain boundaries. Silicon can form a glassy layer that surrounds the zirconia grains. There are some controversies regarding the nature of this layer. Some authors claim that the formation of a continuous glassy layer takes place and subsequently oxygen ion transport across grain boundaries must proceed through this isolating layer [11,12]. Other authors assert only partial wetting of grain boundaries by the silica phase with some direct grain-to-grain contact [13-15]. If this explanation is true, oxygen ion conduction takes place through direct contact between grains [16].

The second explanation of the blocking effect is the presence of electrical potential at grain boundaries, which results in barrier (Schottky barrier) to ion transport. According to Guo and Zhang [10] the grain boundary region is depleted of oxygen vacancies, and this is the reason for the blocking phenomenon in grain-to-grain contact [17].

Many efforts have been made to reduce the blocking effect in Y-TZP. It was found that the alumina added to the zirconia material acts as the silicon scavenger [18-20]. However, the effect of such an addition on the electrical properties of the zirconia solid electrolyte is debated. Some authors [21-23] claim that alumina additions have a beneficial effect on conductivity, while others [24-26] have observed a decrease in electrical conductivity.

As can be deduced from the above short review, the role of alumina addition on the blocking effect in the tetragonal zirconia is still controversial. Moreover, taking into account the promising application of the tetragonal zirconia, mainly as a solid electrolyte in the intermediate temperature solid oxide fuel cells (IT-SOFC), the effect of added alumina on grain growth should be analyzed.

Therefore, the purpose of this work was to determine the dependence of alumina content on both structural and electrical properties of 3Y-TZP.

2. EXPERIMENTAL

2.1. Preparation of TZP

3 mol.% Y_2O_3 - ZrO_2 solid solution powder was prepared using the coprecipitation method and then heated at 800°C for 2 hrs (the powder preparation procedure is described in detail in [27]). The powder was ball milled for 4 hrs and then in an attritor grinder for 8 hrs.

2.2. Modification of grain boundaries of alumina

Y-TZP micropowders with 0.25 mol.%, 0.5 mol.% and 1 mol.% alumina contents were obtained using the coprecipitation-calcination method. Y-TZP powder was soaked in aluminum nitrate aqueous solutions of appropriate concentrations. The suspensions of ZrO_2 and $Al(NO_3)_3$ were stirred using a magnetic stirrer at room temperature. These suspensions were evaporated to dry powders. The powders were then dried and calcinated at 800°C for 2 hrs, and pressed uniaxially under 150 MPa and then consequently isostatically under 350 MPa pressure into pellets. These pellets were sintered in air at alternated temperatures of 1500 or 1550°C for 2 hrs.

2.3. Microstructure observations

The images of the microstructures of sintered samples were studied using the SEM technique (Nova 200 NanoSEM, FEI Company). For morphological observations the samples were polished and subsequently thermally etched at 1400°C for 1 hr. Such a procedure allowed grain boundaries to be revealed and was useful for grain size and shape determination. Relatively low etching temperature preserved the grain growth during this process. SEM images after binarization were processed using Image J 3.14 program. This analysis yielded the quantitative estimates of grain size and shape.

The energy dispersive X-ray spectrometer (Oxford Instruments) coupled with scanning electron microscopy was used to determine the chemical composition of the samples. The analysis was focused on alumina distribution.

2.4. Impedance measurements

Before measurements of conductivity, Pt-paste was applied as the electrode and the samples were heated at 800°C for 2 hrs. The conductivity of Y-TZP pellets and Y-TZP- Al_2O_3 composites was measured in laboratory air at 550, 600, 650, 700 and 750°C. The conductivity was measured by means of impedance spectroscopy using a computer-controlled Solartron (FRA 1260 and dielectric interface 1294). The impedance spectra were analyzed using the ZPLOT software package provided by Solartron. The measurements were performed within the 0.1 Hz-1 MHz frequency range and the amplitude of the sinusoidal voltage was 10 mV.

3. RESULTS

3.1. Microstructure

The detailed description of microstructure is very important for characterization of both electrical and mechanical properties of sintered bodies. These properties are strongly affected by porosity, grain size, grain shape and distribution.

Typical SEM micrographs of the samples sintered at 1500 and 1550°C are illustrated in Figs 1 and 2, respectively. All samples exhibited comparable grain structure. Differences in size and shape (detailed data collected in the Table 1) arose due to different sintering temperatures.

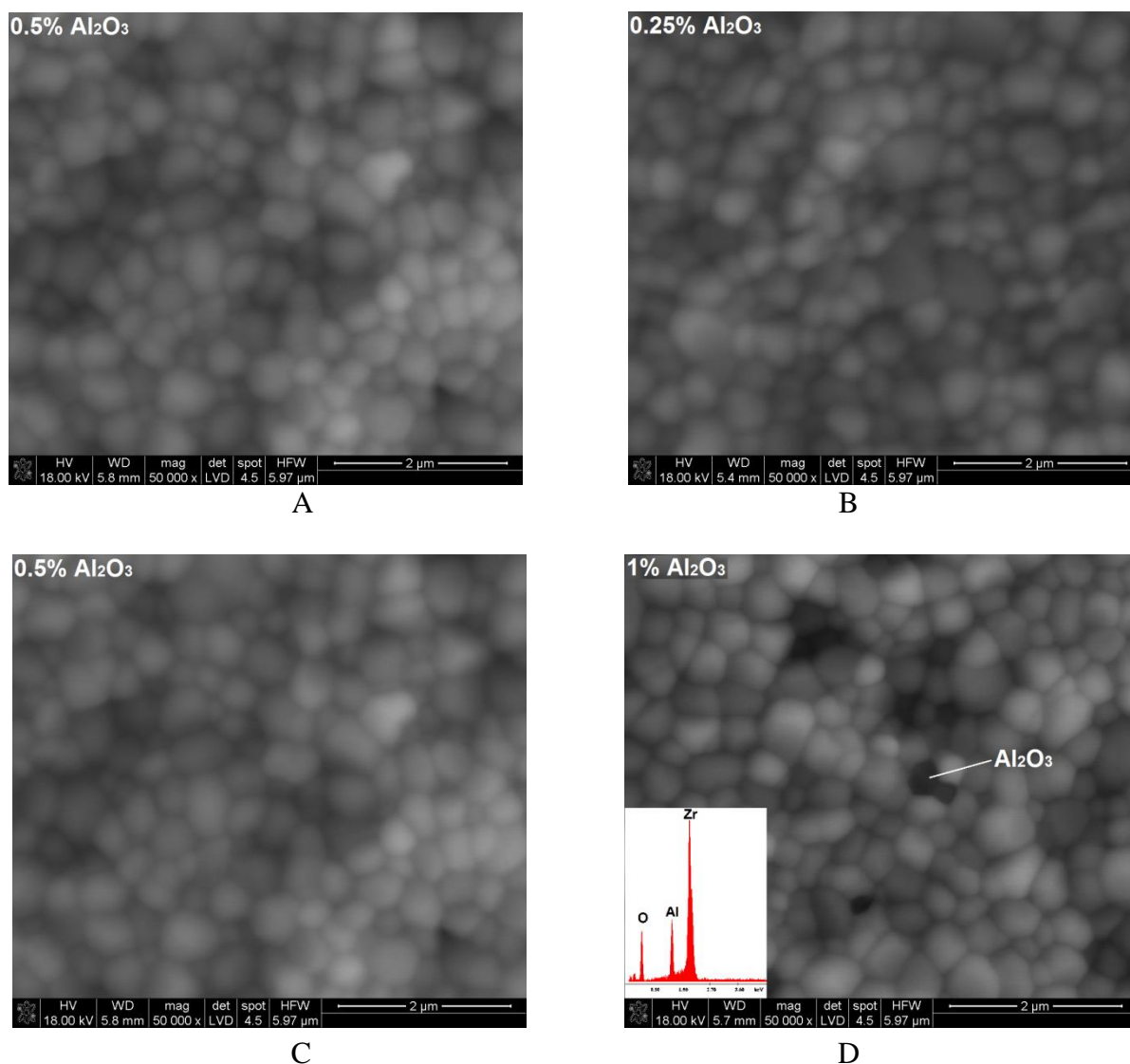


Figure 1. Typical SEM images of microstructures of samples sintered at 1500°C. Alumina content is marked in the upper left-hand corner of the SEM image. EDX spectrum indicates alumina presence in the grain indicated with a white line.

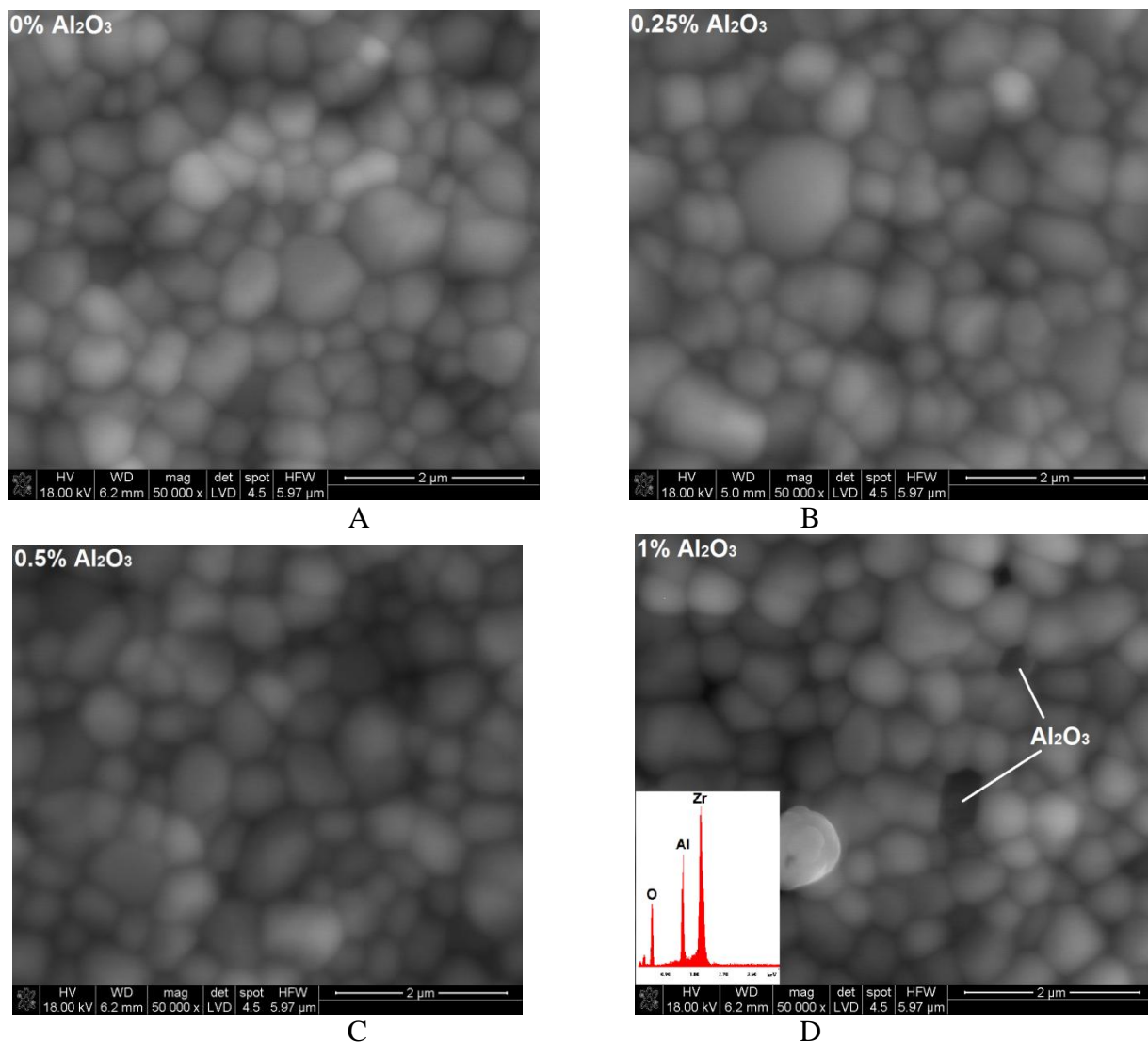


Figure 2 Typical SEM images of microstructures of samples sintered at 1550°C. Alumina content is marked in the upper left-hand corner of the SEM image. EDX spectrum indicates alumina presence in grains indicated with white lines.

Table 1. Mean grain size and grain circularity of sintered bodies.

	Sintering temperature, °C	Alumina content, mol.%			
		0	0.25	0.5	1.0
Mean grain size, μm	1500	0.551 ±0.182	0.478 ±0.200	0.384 ±0.188	0.487 ±0.199
	1550	0.678 ±0.316	0.653 ±0.308	0.608 ±0.310	0.832 ±0.404
Circularity	1500	0.728 ±0.120	0.714 ±0.108	0.641 ±0.146	0.698 ±0.140
	1550	0.686 ±0.129	0.698 ±0.134	0.687 ±0.172	0.600 ±0.163

The smallest average grain size was observed for samples containing 0.5 mol.% of alumina (Fig. 3). It is worth to notice that individual alumina grains could be detected only in the sample prepared with a 1 mol.% Al₂O₃ addition. This was observed for both sintering temperatures.

Samples with 0.5 mol.% alumina content also have the lowest circularity, especially the one sintered at the lower sintering temperature (1500°C). The determined circularity factor has important impact on observed by Pawlowski et al [28] grain boundary migration in zirconia materials. A driving force of the grain boundary migration is a curvature of the grain boundary [28] (which is correlated with circularity factor). Taking into account this phenomenon, the grain boundary structure of the zirconia materials should be treated as no static state but rather as a dynamic state.

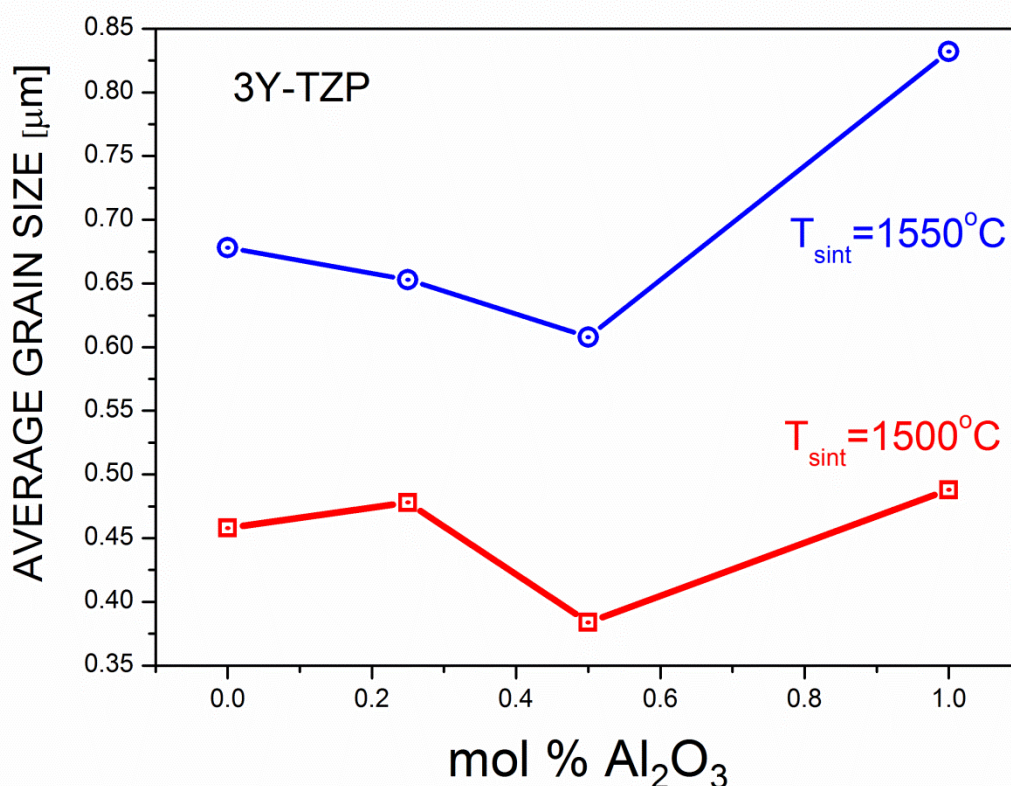


Figure 3. Average grain size vs. alumina content of sintered bodies achieved at both applied temperatures

3.2. Impedance spectroscopy

Fig. 4 shows Nyquist plots of EIS data obtained at five different temperatures for 3Y-TZP sintered at 1500°C. Two parts of semicircles may be distinguished. It is generally accepted [29] that the high-frequency part of the spectrum is related to the specific electrical conductivity of zirconia grains (σ_b) and the low-frequency semicircle describes electrical conductivity of grain boundaries (σ_{gb}), resulting from the blocking effect of charge carriers due to internal interfaces of the material such as grain boundaries, insulating inclusions of impurities and other microstructural defects like pores.

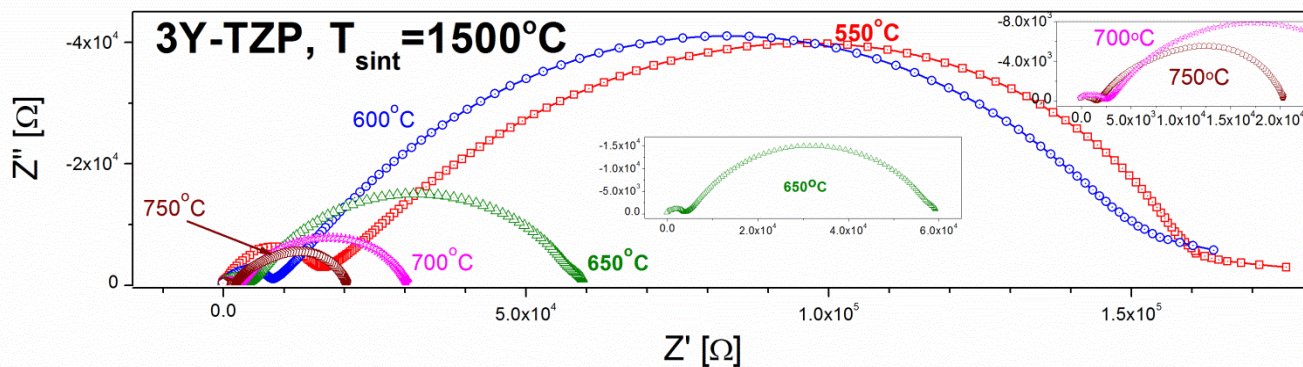


Figure 4. Nyquist plots of EIS data obtained at five different temperatures for 3Y-TZP sintered at 1500°C.

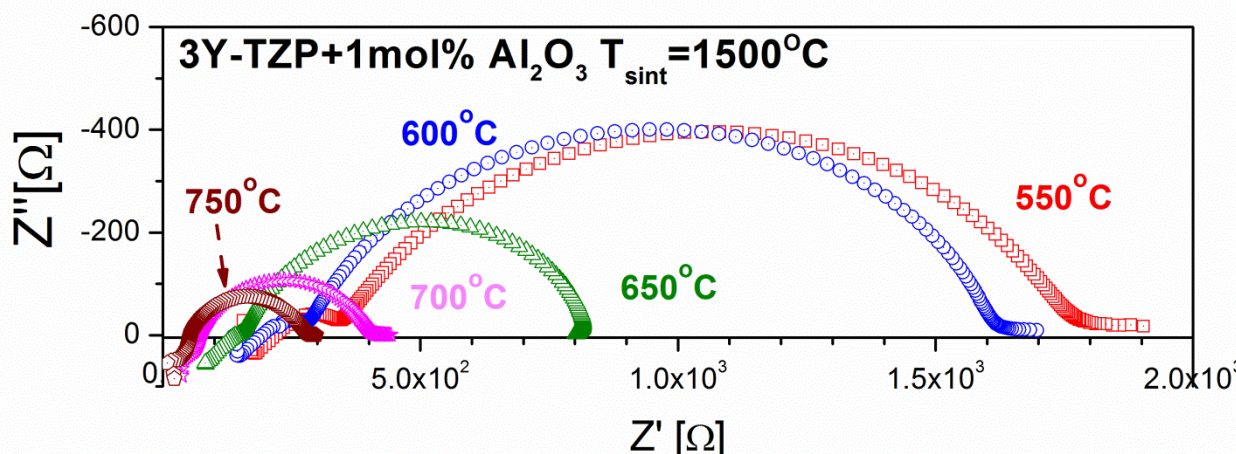


Figure 5. Nyquist plots of EIS data obtained at five different temperatures for 3Y-TZP+1 mol.% Al₂O₃ sintered at 1500°C.

Fig. 5 shows the typical impedance spectra registered at several temperatures for Al₂O₃-modified 3Y-TZP sintered at 1500°C. As in the case of undoped 3Y-TZP, two parts of semicircles can be distinguished. However, the imaginary part of impedance (Z'') assumes positive values at high frequencies. This indicates the contribution of inductance element. Taking into consideration the fact that the impedance of the samples containing alumina is about two orders of magnitude lower than that of non-modified 3Y-TZP, the presence of the inductance element may be attributed to the metallic connections of the sample holder rather than to the sample itself. The observed inductance is therefore disregarded in further analysis. The equivalent circuit used for the fitting of the experimental analysis is presented in Fig. 6. The constant phase element (CPE) is commonly observed instead of Debye's capacitor in the case of polycrystalline samples due to material inhomogeneity, porosity, electrode roughness and ionic transport deviation from Fick's law [30].

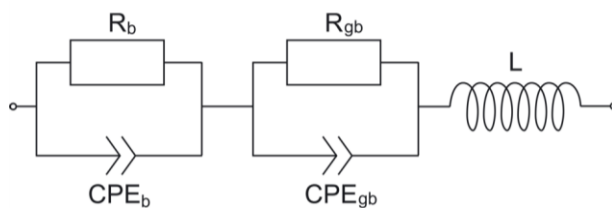


Figure 6. Equivalent circuit used for fitting of experimental data.

4. DISCUSSION

Y-TZP is a candidate for application as an electrolyte in oxygen sensors and fuel cells because of its excellent thermo-mechanical properties [11] and its ionic conductivity, which is comparable or better than that of YSZ [31].

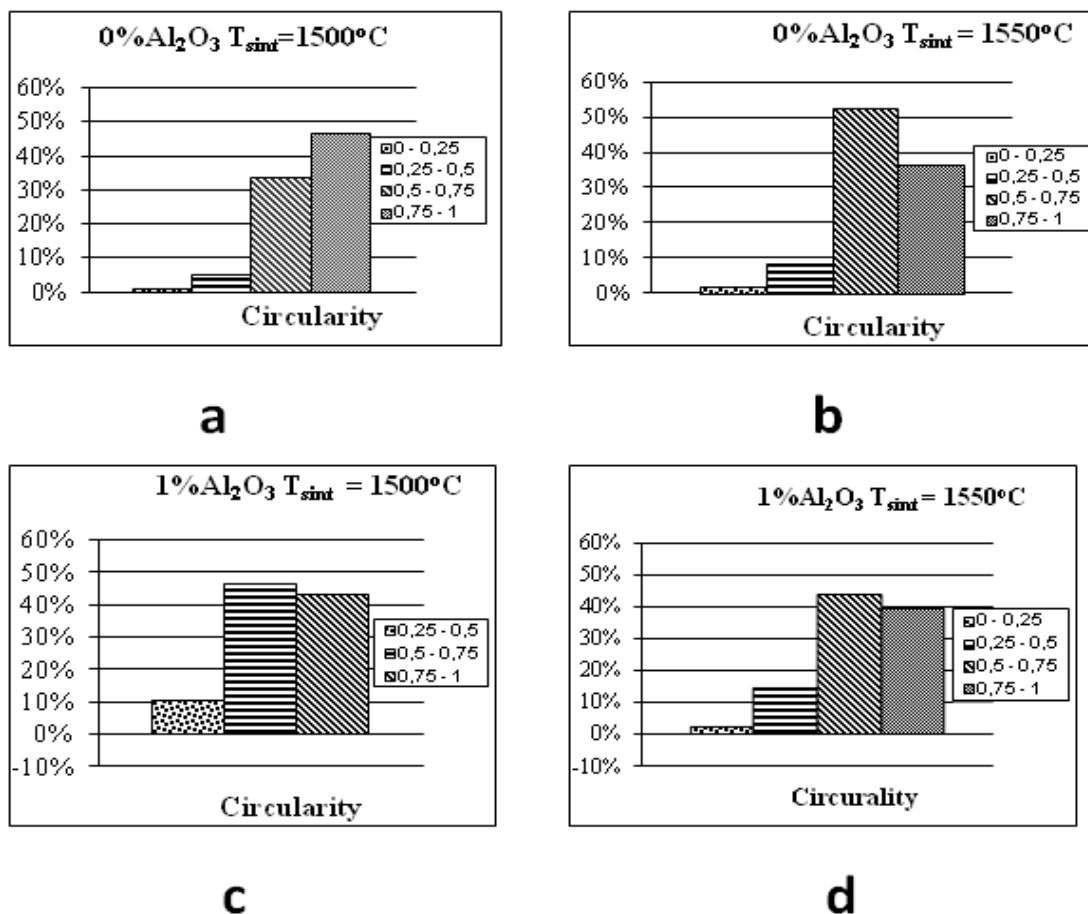


Figure 7. Circularity of grains: a- 3Y-TZP sintered at 1500°C; b- 3Y-TZP sintered at 1550°C; c- 3Y-TZP+1 mol.% Al₂O₃ sintered at 1500°C; d- 3Y-TZP+1 mol.% Al₂O₃ sintered at 1550°C.

However, these materials can undergo phase transformation from tetragonal to monoclinic when annealed at relatively low temperatures [32]. This results in the degradation of both mechanical

properties and electrical conductivity [33], which occurs most extensively at temperatures of 200-300°C, and is related to grain size [34]. When grain size exceeds a critical value the degradation process is remarkable; on the other hand, Y-TZP materials containing smaller grains are stable. The critical grain size for 3Y-TZP is ca. 0.3 μm [35]. A detailed analysis of the shape and size of grains for Y-TZP and Y-TZP+1 mol.% Al₂O₃ is presented in Figs 7 and 8, respectively. The shape of grains is mostly circular (0.75- 1.0 circularity assumes value ca 40 %). The average grain size varies between 0.38 and 0.83 μm (Fig. 3). According to Fig. 8 the sample containing 0.5 mol.% Al₂O₃ and sintered at 1500°C should be the most stable.

The effect of aluminum oxide particles added to solid electrolytes was first investigated by Liang in 1973 [36]. This author observed a considerable increase in total electrical conductivity of lithium iodide after addition of the aluminum oxide powder. Unfortunately, grain interior and grain boundary electrical conductivity components were not determined.

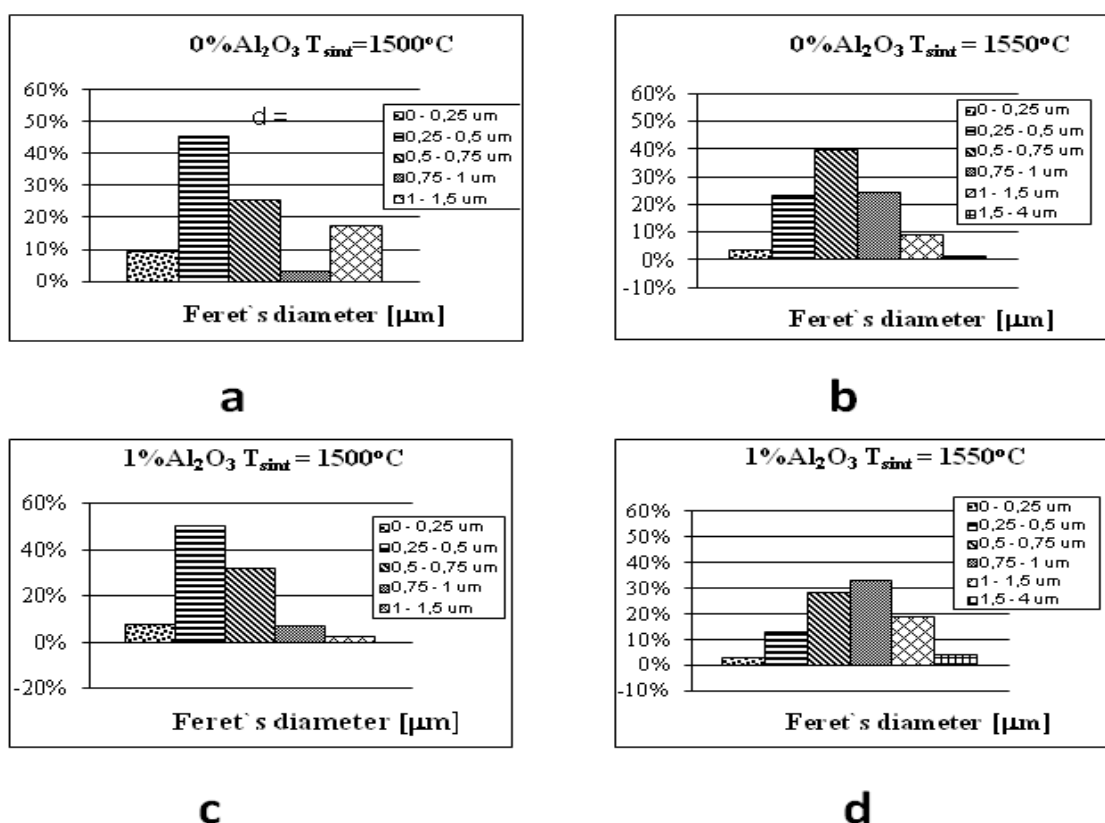


Figure 8. Distribution of grain size: a- 3Y-TZP sintered at 1500°C; b- 3Y-TZP sintered at 1550°C; c- 3Y-TZP+1 mol.% Al₂O₃ sintered at 1500°C; d- 3Y-TZP+1 mol.% Al₂O₃ sintered at 1550°C.

Since impedance spectroscopy enables the measurement of the grain interior and grain boundary resistance and capacitance, it is an important tool for the evaluation of ionic conductivity of zirconia. Grain boundaries significantly affect the properties of polycrystalline ceramic materials such

as Y-TZP, and detailed knowledge of grain boundary behaviour is essential for the optimisation of material properties [37].

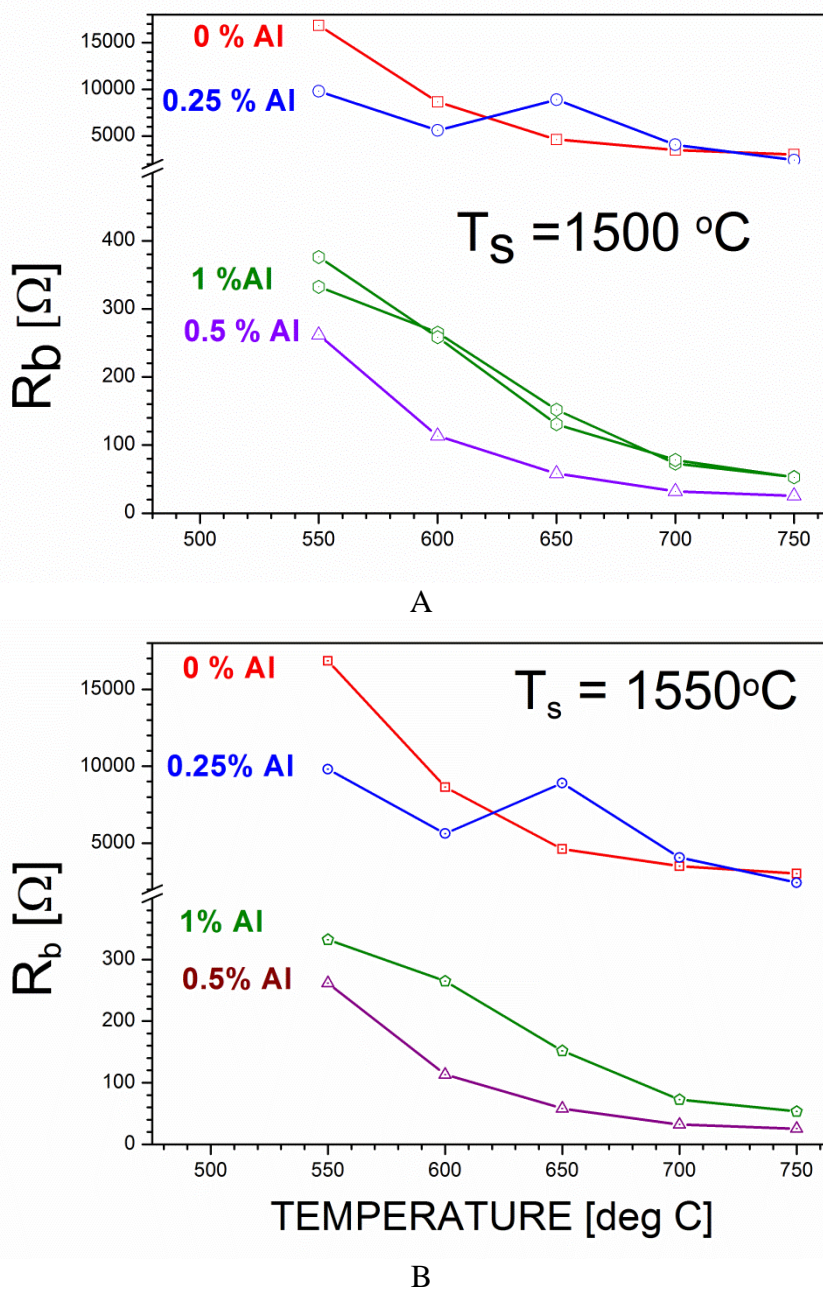


Figure 9. Effect of alumina content on grain resistivity; a- samples sintered at 1500°C; b- samples sintered at 1550°C.

Fig. 9 presents grain interior resistivity versus alumina content for the samples sintered at 1500°C (Fig 9a) and 1550°C (Fig 9b). There are substantial differences between these two sets of dependencies. The addition of alumina to the Y-TZP and then sintering at 1500°C leads to a decrease in grain resistivity. The most pronounced effect is observed in the case of 0.5 mol.% alumina (around 64 and 120 times lower resistivity with respect to undoped Y-TZP at 550 and 750°C, respectively). On

the other hand, the opposite effect of alumina on grain resistivity is observed in the case of the samples sintered at 1550°C (Fig 9b).

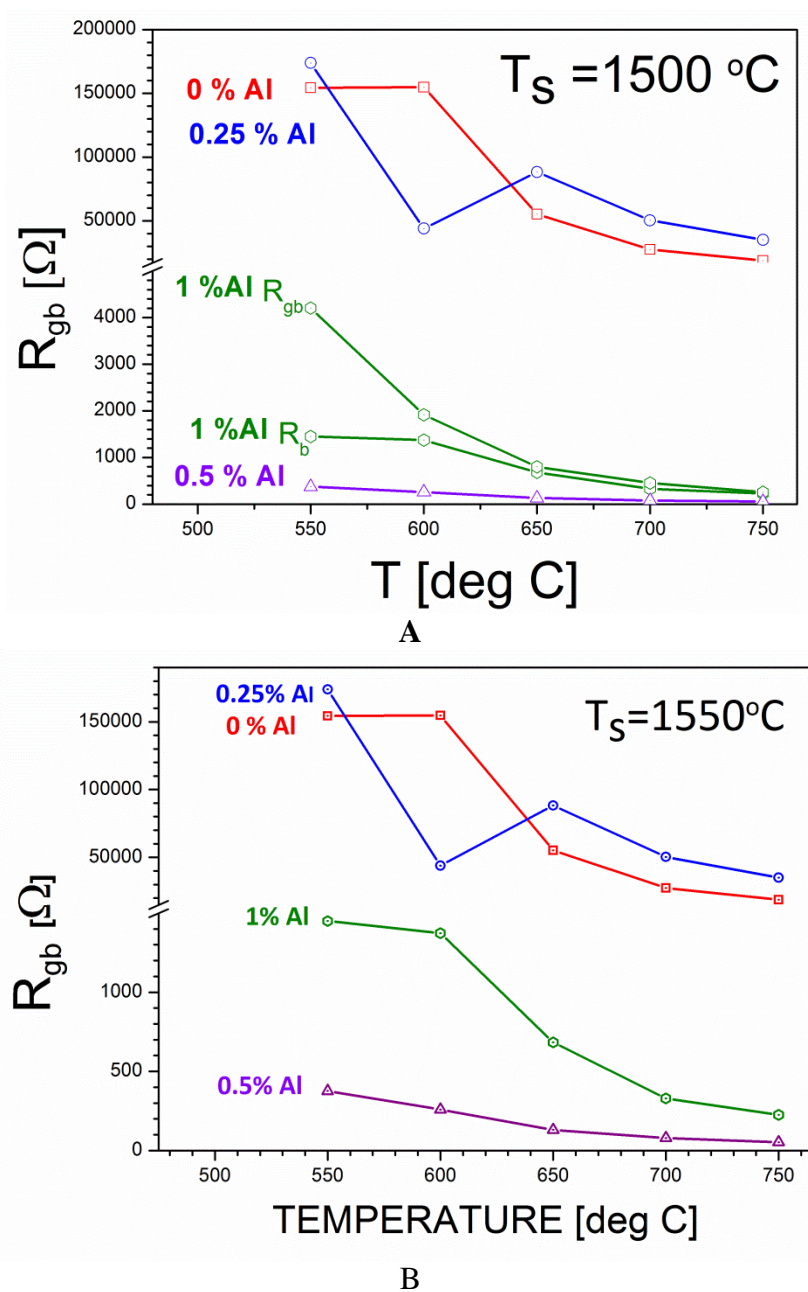


Figure 10. Effect of alumina content on grain boundary resistivity; a- samples sintered at 1500°C; b- samples sintered at 1550°C.

Fig. 10 presents grain boundary resistivity versus alumina content. The observed effects of alumina addition on electrical resistivity of the grain boundaries are similar to those in the case of grain resistivity. Again, the sample containing 0.5 mol.% of alumina and sintered at 1500°C exhibits the lowest grain boundary resistivity.

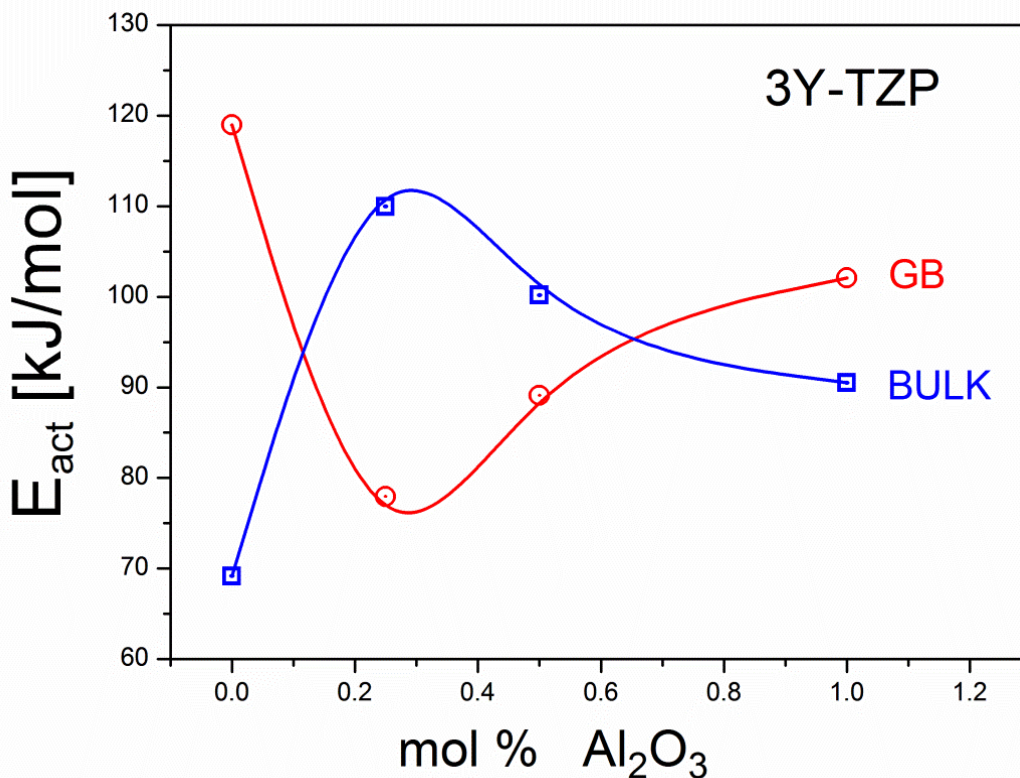


Figure 11. Activation energy of the grains’ electrical conductivity (BULK) and of the grain boundary conductivity (GB) of the samples sintered at 1500°C versus alumina content.

Fig. 11 illustrates the activation energy of electrical conductivity as a function of the concentration of alumina for the samples sintered at 1500°C. The sample containing 0.5 mol.% of alumina exhibits the highest activation energy of bulk electrical conductivity and the lowest activation energy of grain boundary conductivity.

The contribution of grain boundary resistivity to the total resistivity can be determined through the blocking factor (f_R) [13]

$$f_R = \frac{R_{gb}}{R_b + R_{gb}} \tag{1}$$

where R_b and R_{gb} are bulk and grain boundary resistivities, respectively. This factor determines the ratio of the number of electric carriers being blocked at the interfaces under the conditions of the measurements to the total number of electric carriers in the sample.

Fig.12 presents the blocking factor as a function of alumina concentration at several temperatures. The blocking factor assumes the lowest values for the sample containing 0.5 mol.% Al₂O₃.

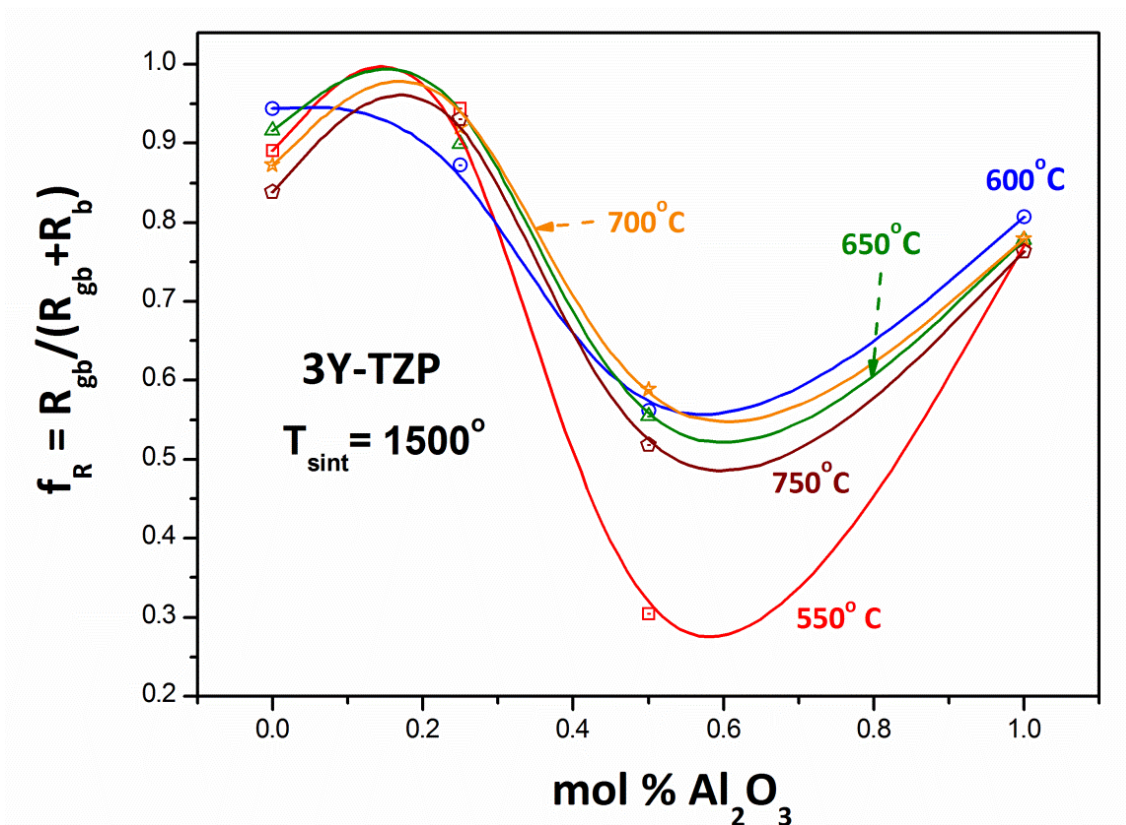
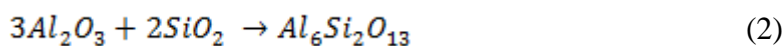
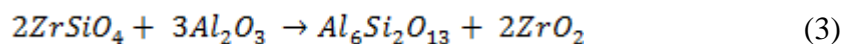


Figure 12. The blocking factor ($f_R = R_{gb}/(R_{gb}+R_b)$) parameter as a function of alumina concentration at several temperatures.

There are two main explanations of the observed effect of alumina additions on the electrical conductivity of 3Y-TZP. The first one, named the ‘scavenger’ model, assumes that the low grain boundary conductivity of 3Y-TZP is attributed to intergranular siliceous phases, which wet the grain boundaries. The added alumina reacts with silica, forming a stable mullite:



According to Butler and Drennan’s [18] thermodynamic calculations reaction (2) is possible when the activity of silica is at least 0.03 at 1600°C. On the other hand, the reaction between zirconia and silica yields the unstable silicate $ZrSiO_4$, which dissociates above 1540°C. However, this compound is not stable in the presence of alumina:



The Gibbs free enthalpy of reaction (3) is negative above 920°C. The alumina/mullite system act as a buffer for silica, absorbing SiO_2 from any sources where it is present and exhibits higher activity than 0.03 [18]. Consequently, alumina acts as a silica scavenger.

The presented scavenger model provides a fitting explanation of the improvement in grain boundary conductivity, but is unable to explain the increase in bulk electrical conductivity observed

after the addition of the alumina. Moreover, according to Verkerk et al. [22] and Guo [38], zirconia materials of high purity in which the siliceous phase was not observed, the specific grain boundary conductivity was still ca. 2 orders of magnitude lower than that of the bulk.

The second model that explains the effect of addition alumina on the electrical properties of zirconia materials, reported by Guo et al. [38-40], is based on a Schottky barrier model. According to this model aluminum ions incorporate into the zirconium sublattice, forming defect associates with oxygen vacancies. The space-charge depletion layer which is correlated with grain size plays an important role in electrical conductivity.

5. CONCLUSIONS

The effect of adding various amounts of aluminum oxide and the influence of sintering temperature on both the microstructure of ZrO_2 containing 3 mol.% Y_2O_3 (3Y-TZP) and its electrical properties have been studied. The investigation revealed that the 3Y-TZP sample that contained 0.5 mol.% Al_2O_3 and was sintered at 1500°C shows the most desirable microstructure (smallest average grain size) and the highest electrical conductivity. This effect can be explained not only by the minimization of grain boundary resistivity as a result of the so-called scavenger effect but also by the improvement in total electrical conductivity.

ACKNOWLEDGEMENTS

The financial support of the Institute of Power Engineering, Strategic Project NCBiR (grant no. OZE/2/2010) is gratefully acknowledged.

References

1. K. Kobayashi, H. Kawajima, T. Masaki (1981), *Solid State Ionics*, 3/ 4 (1981) 489
2. T.K.Gupta, J.H. Bechtold, R.C. Kuznick, L.H. Cadoff, B.R.Rossing, *J.Mater.Sci.*, 12 (1977) 2421
3. T.K. Gupta, R.B. Grekila, E.C. Subbaro, *J.Electrochem.Soc.*, 128 (1981) 929
4. R.C. Garvie, R.H.J. Hannik, R.T. Pascoe RT, *Nature* (London), 258 (1975) 703.
5. S.P.S. Badwal, *Appl.Phys.A* 50 (1990) 449
6. S.P.S. Badwal, J. Drennan, *J.Mater.Sci.*, 24(1989) 88
7. S.P.S. Badwal, M.V. Swain, *J.Mater.Sci.Lett.* 4 (1985) 487
8. N. Bonanos, R.K. Slotwinski, B.C.H. Steele, *J.Mater.Sci.Lett.*, 3 (1984) 245
9. D. Meyer, U. Eisele , R. Satet, J. Rödel, *Scripta Materialia*, 58 (2008) 215
10. X. Guo, Z. Zhang , *Acta Mater.* 51 (2003) 2539
11. M. Rühle, N. Claussen, A.H. Heuer, *Sci.Technol.Zirconia II, Adv.Ceram.*, 12 (1984) 352
12. J. Tanaka, J.F. Baumard, P. Abelard, *J.Am.Ceram.Soc.*, 70 (1987) 637
13. A.E. Hughes, S.P.S. Badwal , *Materials Forum*, 15 (1999) 261
14. T. Stoto, M. Neuer, C. Carry *J.Am.Ceram.Soc.*, 74 (1991) 2615
15. T. Masaki, K. Sinjo, *Ceram.Intern.*, 13(1987) 109
16. S.P.S. Badwal , *Solid State Ionics*, 76 (1995) 67
17. A.P. Santos, R.Z. Domingues, M. Kleitz , *J.Europ.Ceram.Soc.*, 18 (1998) 1571
18. E.P. Butler, J. Drennan, *J.Am.Ceram.Soc.* ,65 (1982) 474

19. A.J. Feighery, I.T.S. Irvine, *Solid State Ionics*, 121 (1999) 209
20. M.C. Martin, M.L. Mecartney, *Solid State Ionics*, 161(2003) 67
21. E.P. Butler, R.K. Slotwinski, N. Bonanos,, J. Drennan, B.C.H. In Claussen N, Ruhle M, Heuer AT (eds) *Sci. Tech. of Zirconia II, Advances in Ceramics v. 12*, Am.Ceram.Soc (1984) , Columbus , OH, p. 572
22. M.J. Verkerk, A.J. Winnubst, A.J. Burggraaf, *J.Mater.Sci.*, 17 (1982) 3113
23. S.P.S. Badwal, W.G. Garret, M.J. Bannister, *J.Phys.E: Sci. Instrum.*, 20 (1987) 531
24. M. Miyayama, H.Y. Yanagida, *Am.Ceram.Soc.Bull.*, 64 (1985) 660
25. K. Yamana, W. Weppner, A. Kopp, T. Yoshimura , *J.Mater.Sci.Lett.* 10 (1991) 1201
26. S. Nazarpour, C. Lopez-Gandara, F.M. Ramos, A. Cierera, *J.Alloys Compounds*, 505 (2010) 527
27. E. Drozd-Ciesla, J. Wyrwa, W. Pyda, M. Rekas,, *J.Mater.Sci.*, 47 (2012) 2807
28. A. Pawlowski, M.M. Bucko, Z., *Mater.Res.Bull.*, 37(2002) 425
29. J.E. Bauerle, *J.Phys.Chem. Solids*, 30 (1969) 2657
30. J.R. Macdonald, in *Impedance Spectroscopy-Theory, Experiment and Applications*, Wiley, New York p. 191 (1987)
31. S.P.S. Badwal, *J.Mater.Sci.Lett.*, 6 (1987) 1419
32. R.A. Rocha, E.N.S. Muccillo, L. Dessemond, E. Djurado, *J.Europ.Ceram.Soc.*,30 (2010) 227
33. D-J. Kim, H-J. Jung, J-W. Jung, H-L. Lee , *J.Am.Ceram.Soc.* ,81(1998) 2309
34. S. Lawson S , *J.Europ.Ceram.Soc.* ,15 (1995) 485
35. M. Watanabe, S. Iio, I. Fukurara , In N. Claussen, M. Ruhle, A.H. Heuer, (eds).*Advances in Ceramics vol. 12 Science and Technology of Zirconia II*, The American Ceramic Society, Inc. Columbus, Ohio pp. 391 (1984).
36. C.C. Liang, *J.Electrochem.Soc.*, 120 (1973) 1289
37. C.R. Bowen, A.W. Tevernor, J. Luo, R. , *J.Europ.Ceram.Soc.*, 19(1999) 149
38. X. Guo, *Phys.Stat.Sol. (a)*, 183(2001) 261
39. X. Guo, W. Sigle, J. Fleig, J. Maier, *Solid State Ionics*, 154-155 (2002) 555
40. X. Guo, R. Waser, *Prog.Mater.Sci.*, 51 (2006) 151.